CHAPTER II

DESCRIPTION OF EXPERIMENTAL APPARATUS FOR THREE-PHASE FLUIDIZED BED

2.1 Introduction

Over the past ten years, extensive experimental research on two-phase fluidization systems, which consisted of only gas and solid phases, has been carried out at the Illinois Institute of Technology (IIT) by a number of researchers (Miller and Gidaspow, 1992; Gamwo, 1992; Seo and Gidaspow, 1987; Gidaspow and Ettehadieh, 1983 and others). These experiments led to a better understanding of the hydrodynamics of both the bubbling fluidized beds (Seo and Gidaspow, 1987; Gidaspow and Ettehadieh, 1983; Gamwo, 1992), and the circulating fluidized beds (Miller and Gidaspow, 1992). The experimental research was vital to the development and extension of predictive hydrodynamic models to multiphase flows and fluidization at IIT.

However, for the first time, the experimental work on gas-liquid-solid fluidization, gas-liquid fluidization and liquid-solid fluidization is undertaken at IIT. The experiments involve the measurements of the bubble sizes, time average volume fractions, instantaneous porosity fluctuations, particle velocity measurements, and bed viscosity measurements. The results of these experiments were also used to validate existing multiphase hydrodynamic models for gas-liquid-solid, liquid-solid and gas-liquid fluidization systems (Jayaswal, 1991). These hydrodynamic models could be used as cost-effective design and troubleshooting tools by industries.

2.2 Experimental Apparatus and Procedure

The apparatus used in this experiment consisted of two major components : the fluidization equipment, and the densitometer assembly. A schematic diagram of the apparatus is shown in Figure 2.1.

2.2.1 Fluidization Equipment. A two-dimensional bed was constructed from transparent acrylic (plexiglas) sheets to facilitate visual observation and video recording of the bed operations such as gas bubbling and coalescence, and the mixing and segregation of solids. The bed height was 213.36 cm and cross-section was 30.48 cm by 5.08 cm. A centrifugal pump was connected to the bottom of the bed by a 1.0 inch (2.54 cm) I.D. stainless steel pipe. A compressor was connected to the sides of the bed. Liquid was stored in and recycled back to a fifty-five gallon storage tank.

The liquid and gas distributors were located at the bottom of the bed. The liquid was distributed by two perforated plexiglas plates with many 0.277 cm diameter holes. They were placed at 35.56 cm and 50.8 cm above the bottom of the bed, with 0.25 cm size glass bead particles filling the inside. The gas distributor consisted of six staggered 15.24 cm long porous tubes of 0.28 cm diameter. The fine pores of porous tubes had a mean diameter of 41.88 μm. The porous tubes were placed at the bottom of the bed between the liquid distributor.

2.2.2 Densitometer Assembly. Two densitometers were used alternatively for measuring both the time-averaged and the instantaneous volume fractions of three phases by means of the x-ray and γ-ray adsorption techniques. The assembly consisted of radioactive sources as well as detecting and recording devices and a positioning table.

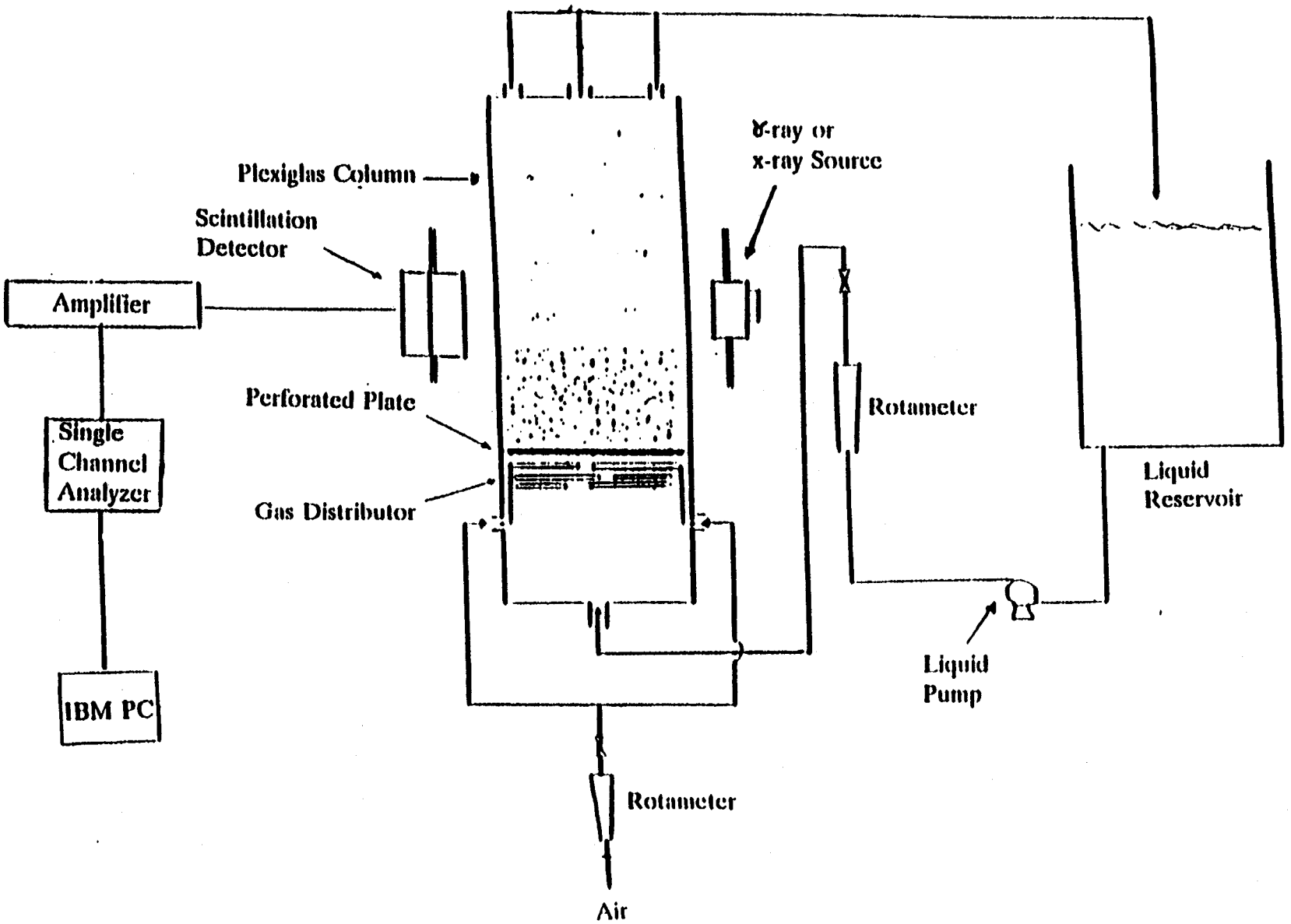

Figure 2.1. Schematic Diagram of the Experimental Apparatus

A schematic diagram of the detector and recording devices assembly is shown in Figure 2.2.

2.2.2.1. Radioactive Source. The souree is a 200-mCi Cu-244 having a 17.8-year half-life. It emitted X-rays with a photon energy between 12 and 23 keV. The source was contained in a ceramic enamel, recessed into a stainless steel support with a tungsten alloy packing, and sealed in a welded Monel Capsule. The device had a brazed Beryllium window. For the γ-ray densitometer, a 20-mCi Cs-137 source having a single γ-ray energy of 667 kev and a half-life of 30 years was used. The source was sealed in a welded, stainless steel capsule. The source holder was welded, filled with lead, and provided with a shutter to turn off the source. This is the same unit we used previously (Gidaspow et al., 1983).

2.2.2.2. Detecting and Recording Devices. The intensity of the X-ray beam was measured by using a NaI crystal scintillation detector (Teledyne, ST-82-I/B). It consisted of a 2-mm thick, 5.08 cm diameter tube with a 0.13-mm thick Beryllium window. For the γ-ray densitometer, the intensity of the γ-ray beam was detected by another NaI crystal detector (Teledyne, S-44-I/2). The dimensions of the crystal were as follows : 5.08 cm thick and 5.08 cm in diameter. The two detectors could be switched for use with different sources. The photomultiplier of the detector was connected sequentially to a preamplifier, an amplifier and a single-channel analyzer, a rate meter, and a 186 IBM compatible personal computer. The rate meter has a selector and a 0-100-mV scale range.

2.2.2.3. Positioning Table. Both the source holder and detector were

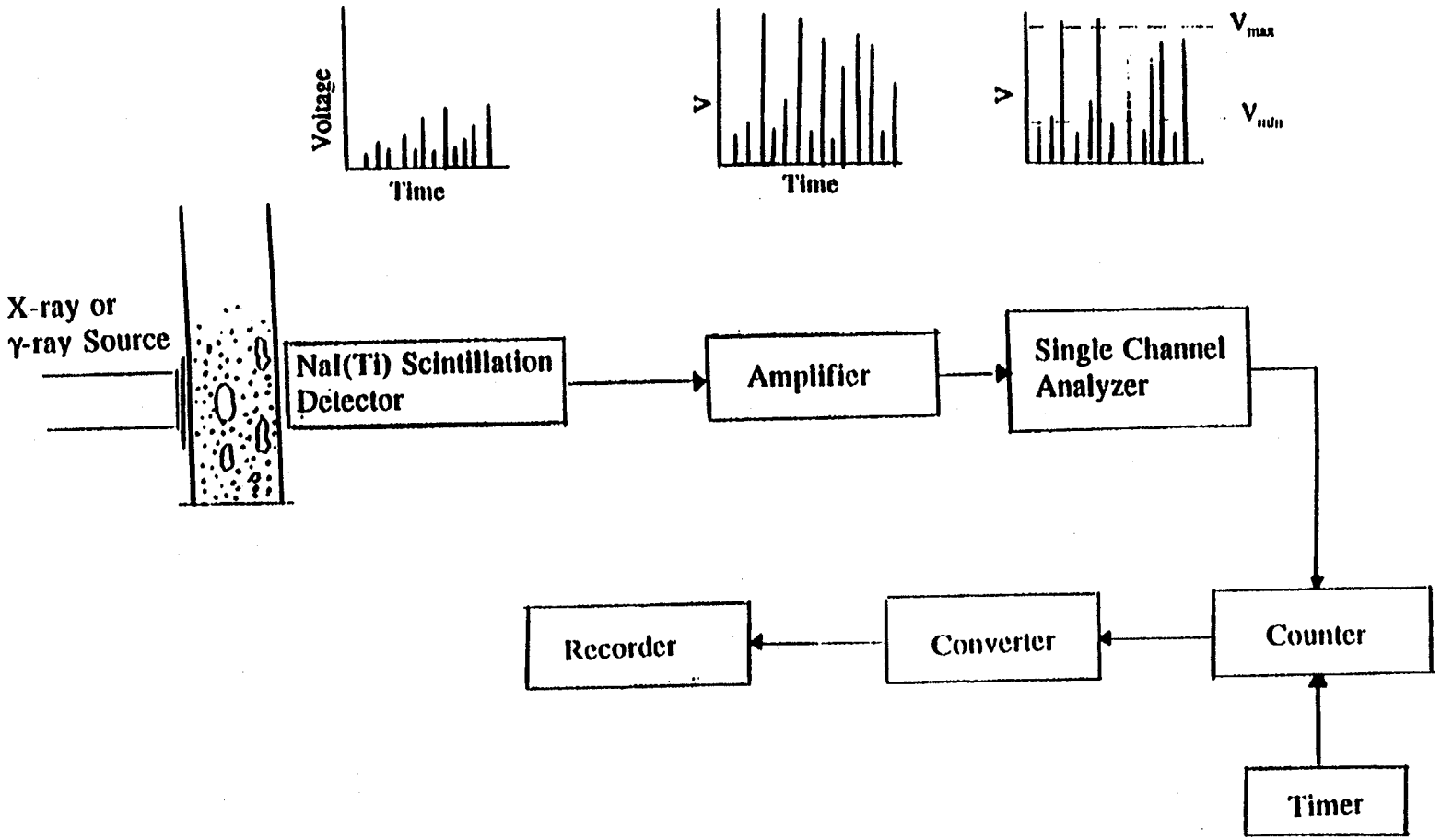

Figure 2.2. Schematic Diagram of Source-Detector-Recorder Assembly for X-ray and γ-ray Densitometer

affixed to either side of the bed on a movable frame and could be moved anywhere up-or-down or back-and-froth by means of an electric motor.

2.2.3. Experimental Procedure. The liquid from the storage tank was fed to the bed from the bottom of the bed using the centrifugal pump. The gas was fed to the bed through a compressor. Both gas and liquid from the top of the bed were directed through three openings of 1.0 inch (2.54 cm) I.D. stainless steel pipes back to the storage tank, where the gas was separated from the liquid.

In order to achieve a uniform fluidization, the liquid distributor section was designed in such a way that the pressure drop through the distributor section was 10-20 % of the total bed pressure drop. The gas was distributed in the fluidized bed through the six staggered porous tubes.

Air and water were used as the gas and liquid, respectively, in this experiment. Ballotini (leaded glass beads) with an average diameter of 800 μm and a density of 2.944 g/cm^3 were used as the solids.

The experimental volume fractions measurements were made at 240 different locations at every 1.27 cm in both -x and -y directions on the left portion of the bed.

The experimental operating conditions are shown in the Table 2.1.

Table 2.1. Experimental Operating Conditions

Temperature	23.5 °C
Pressure Drop	0.083 atm
Initial Bed Height	25.4 cm
Particle Mean Diameter	800 μm (0.8 mm)
Particle Density	2.94 g/cm^3
Minimum Fluidization Velocity	0.76 cm/s
Maximum Packing Porosity	0.39

2.3 Visual Observations of Bubble Coalescence and Break up

The hydrodynamic behavior of a multiphase fluidization system is due to complex interactions between the individual phases, and is also affected by the gas and liquid distributor designs. The phenomenon of bubble behavior at any axial location within a three-phase fluidized bed starts in the distributor region where bubbles are formed. The initial bubble sizes depend on the distributor design as well as buoyancy, viscous drag and surface tension. By using the surface tension equation, Azbal (1981) described the bubble diameter (d_b) at the instant of release as :

$$d_b = \left[\frac{6\sigma D_o}{(\rho_f - \rho_g) g}\right]^{1/3} \qquad (2.1)$$

where ρ_g and ρ_l are the densities of the gas and liquid phases, respectively; D. is diameter of the orifice (42 μm); σ is the surface tension and g is the gravitational constant.

The average bubble diameter at the moment of release from the orifice was calculated to be 0.124 mm. As soon as the bubbles left the orifice the mean bubble sizes were increased with an increase in the axial distance. These changes were also found by Massimilla et al. (1961) and Ostergaard (1969). Fan (1989) described this behavior of the bubble as " bubble coalescence ".

Another behavior of the bubble that Fan (1989) described was bubble break-up. This behavior was also observed in this experiment. He defined this mechanism as an interaction between a bubble and individual particles. According to and Fan (1989):

$$1 > \frac{h\omega^2}{A_{co} - (A_{co}^2 - U_r^2\omega^2)^{\frac{1}{2}}} \qquad (2.2)$$

where,

$$A_{co} = g\frac{\rho_l - \rho_s}{\rho_s} + \frac{6\sigma}{\rho_s d_p^2}\left(1 + \frac{d_p}{2r_o}\right) \qquad (2.3)$$

and

$$\omega = \left(\frac{3}{2}\frac{g}{d_p}\frac{\rho_l}{\rho_s}\right)^{1/2} \qquad (2.4)$$

A particle will penetrate through the bubble if equation (2.2) satisfied. However, this criterion constitutes only a necessary condition for bubble breakup with a single particle. The calculations for our experiment showed that the right hand side of equation

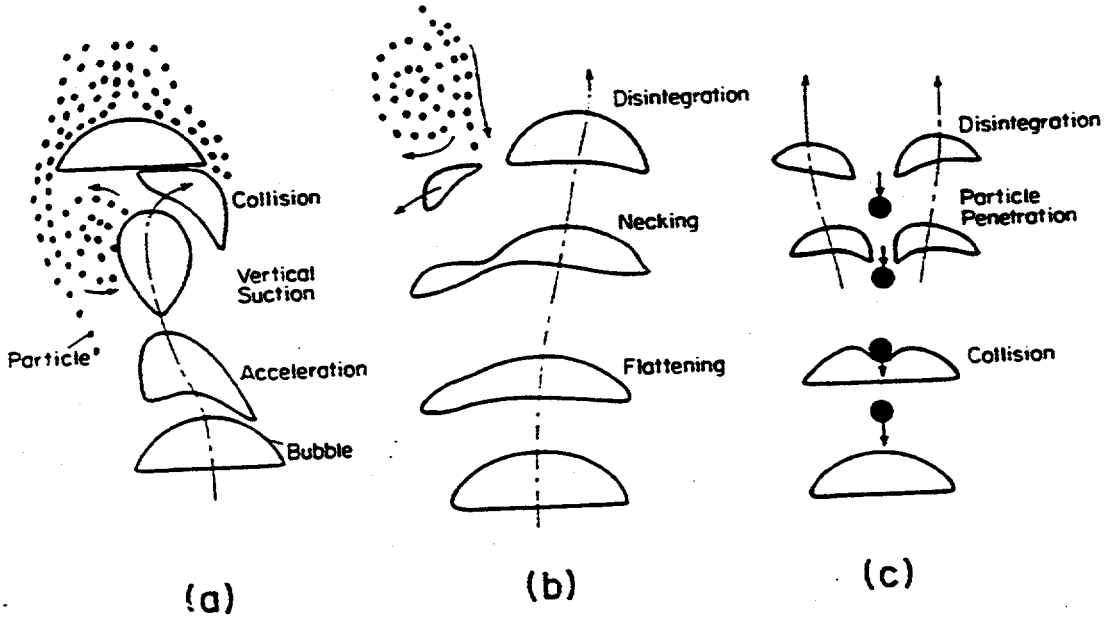

Figure 2.3. Mechanism of Coalescence and Disintegration of Bubbles in Gas-Liquid-Solid Fluidized Beds (Fan, 1989)

(2.2) was 0.28, which is less than 1.0. Therefore particles could penetrate through the bubbles in our fluidized bed, and break up the bubbles as well. Figure 2.3 pictorially shows the mechanism of coalescence and disintegration of bubbles in gas-liquid-solid fluidized beds (Fan, 1989).